INVESTIGATION OF THE THERMAL CONDUCTIVITY OF POROUS CERMET MEMBERS

P. A. Novikov and B. G. Mikhnyuk

UDC 536.2

This article presents data obtained in investigating the thermal conductivity of a porous metal as a function of its porosity and the pressure and nature of the carrier gas.

Porous cooling has come into wide use in various branches of modern engineering. It is employed for cooling jet nozzles, gas-turbine blades, the walls of heat exchangers, etc. and has come to be of particular importance in nuclear power reactors with a gaseous heat-transfer agent (helium, hydrogen, nitrogen, air, freon, steam, etc.), where the heat-transfer characteristics in gas-filled porous cells are of practical importance.

Porous cooling requires use of porous cermets, whose thermophysical properties must be known. We can speak of the thermal characteristics of porous bodies (λ, c_p, a, etc.) only very arbitrarily, using this term to mean the equivalent thermal characteristics that make it possible to obtain an overall notion of the heat-propagation process in the solid.

The thermal conductivity of porous bodies depends on many factors: their porosity, the type of filler, the degree of filling, the temperature, the ambient pressure, etc. However, this relationship has still not been fully covered in the literature, despite the increasing number of studies that have been made in this area. Theoretical attempts to determine the thermal conductivity of porous media yield results suitable only for qualitative evaluation of experimental results, since it is impossible to take the real structure of a porous body into account to a sufficient extent. All quantitative calculations are therefore made on the basis of data obtained experimentally.

The present investigation was conducted to establish the dependence of the thermal conductivity of a porous cermet on its porosity, the total pressure, and the nature of the filler gas.

The thermal conductivity was determined under a steady-state thermal regime. The experimental subject was a round plate bounded by parallel planes. The porous plates were fabricated from powdered metal (titanium) pressed under high pressure and sintered at a temperature close to its melting point. The titanium powder had the following foreign inclusions: 0.06% N_2, 0.04% C, 0.06% Si, 0.21% Fe, 0.07% Ni, and 0.05% Ca. The thermal conductivity of titanium with this impurity content is $\lambda_{sk} \cong 16$ W/m·deg [4]. The powder particles were of arbitary shape (close to spherical) and from 3 to 7 μm in diameter.

In order to use a single plate without a lateral retaining ring, the specimen thickness was small in absolute terms ($\delta = 0.003$ m), while the ratio δ/D was about 1:50.

The experiments were conducted in a vacuum apparatus, which is diagrammed in Fig. 1.

The principal structural elements of the apparatus are a heating element and a condenser. The former was fabricated from Nichrome wire with a diameter of $2 \cdot 10^{-4}$ m wound into a helix with closely spaced turns. The diameter of the heating element was equivalent to that of the specimen and its thickness did not exceed $3 \cdot 10^{-4}$ m. This heating-element design made it possible to reduce lateral heat leakage to a minimum.

The condenser design permitted regulable withdrawal of a given amount of heat per unit specimen surface. In order to ensure good thermal contact between the specimen on one hand and the heating element and condenser on the other, thin vacuum-rubber pads $3 \cdot 10^{-4}$ m thick were placed between them.

Institute of Heat and Mass Transfer, Minsk. Translated from Inzhenerno-Fizicheskii Zhurnal, Vol. 17, No. 4, pp. 655-664, October, 1969. Original article submitted November 22, 1968.

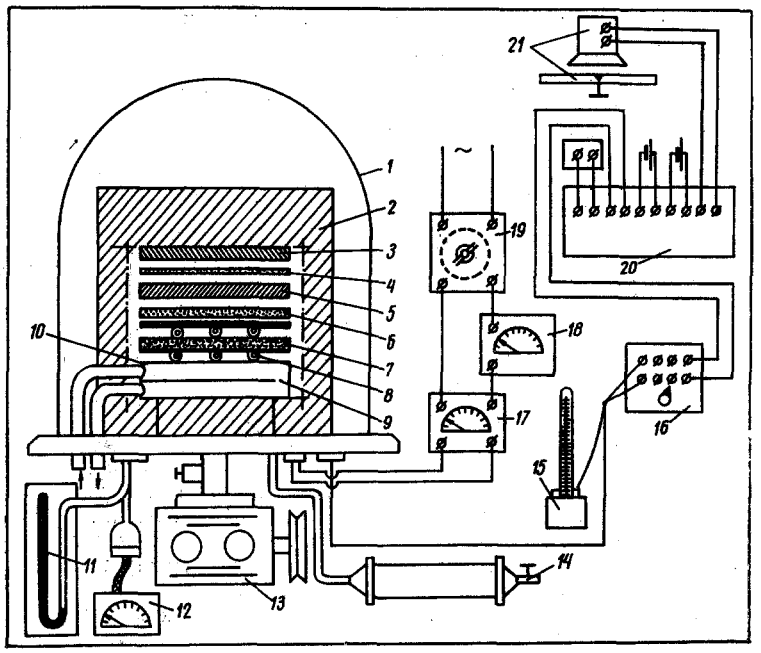

Fig. 1. Diagram of experimental apparatus: 1) glass bell; 2) heat-insulating housing; 3) clamp plate; 4) shielded heating element; 5) organic glass disk; 6) main heating element; 7) porous member; 8) thermocouples; 9) condenser; 10) rubber padding; 11) U-shaped vacuum meter; 12) thermocouple vacuum meter; 13) vacuum pump; 14) drier shell; 15) Dewar flask with cold thermocouple junction; 16) thermocouple switches; 17) voltmeter; 18) ammeter; 19) LATR; 20) low-resistance potentiometer; 21) mirror galvanometer.

In addition to the main heating element, a shielded heating element was provided. The temperature difference between these elements was monitored with two differential thermocouples.

The temperature was determined with eight copper – constantan thermocouples mounted in sets of four opposite one another on either side of the plate (Fig. 1).

Strips of aluminum foil $5 \cdot 10^{-5}$ m thick were wrapped around the heads of the thermocouples on the rubber-pad side, ensuring good thermal contact between the head and specimen and providing an averaged measured temperature.

The specific heat flux q was determined from the known resistance R of the heating element and the current I. The emf of the thermocouples was measured with the aid of a low-resistance potentiometer and a mirror galvanometer with a high accuracy rating. The laboratory instruments made it possible to determine the temperature to within 0.02°C.

In order to verify the research procedure and the accuracy of the experimental apparatus, the first experiments were conducted with standard specimens fabricated from organic glass and cuprite. The experimental results showed that the thermal conductivity of these materials remained unchanged when the pressure was varied and was within the range of tabulated values. This apparatus can thus be used to determine the thermal conductivity of materials with different physical properties, from insulators to heat conductors.

The conductivity meter, consisting of the main and shielded heating elements, the specimen, and the condenser, was assembled in a cassette, which was tightly sealed with tie bolts. It was then enclosed in a protective lateral collar and a heat-insulating shell and installed intact in the vacuum chamber. The pressure in the chamber was adjusted to the desired range, from $1 \cdot 10^5$ to about 1 N/m^2. The apparatus was fitted with a system for adjustable admission of various gases, including saturated water vapor, to the chamber. The gas was delivered through a drier filled with silica gel.

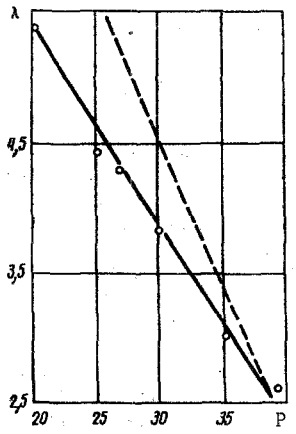

Fig. 2. Coefficient of thermal conductivity of porous cermet element (titanium) λ, (W/m · deg) as a function of porosity Π (%). The dots represent experimental data and the dash curve represents calculated data.

The average specimen temperature was set close to the ambient temperature in order to prevent thermal losses. The time required to establish a steady-state regime under vacuum conditions was about 2 h. The coefficient of thermal conductivity was calculated from the formula

$$\lambda = \frac{QS}{\delta \Delta T} . \tag{1}$$

Figure 2 shows λ(W/m · deg) as a function of the porosity P (%) for titanium cermet elements at T = 290°K under vacuum conditions. It can be seen from this figure that the coefficient of thermal conductivity decreased with increasing material porosity, from λ = 5.4 at Π = 20% to λ = 2.6 at Π = 39%. This same graph shows the function λ = f(Π) (dash line) obtained by calculation from the formula [5]

$$\lambda = \frac{\lambda_{sk}}{0.242} \frac{1 - (\Pi + 0.523)^{1/3}}{(\Pi + 0.523)^{1/3}} \tag{2}$$

for an ideal cermet system, in which the contact thermal resistance equals zero.

As can be seen from this graph, the greatest discrepancy between the experimental and calculated data was observed for the plate with lowest porosity.

We therefore used the same elements, in which the contact resistance could be neglected, in our subsequent experiments with gaseous fillers, in order to preclude the influence of the contact resistance between individual grains. The activity porosity of the cermet elements $\Pi = V_p/V_0$ was determined by the impregnation method.

Before impregnation, the thoroughly purified and dried porous specimen was placed in a hermetic dish, from which the air was evacuated with a vacuum pump. After evacuation of the air from the porous element, a liquid (mercury, benzene, ethanol, water, or ethyl ether) was forced through it under pressure.

The mass of the liquid absorbed by the porous specimen was determined with an analytical balance, from the difference in specimen weight before and after impregnation, i.e.,

$$M_l = m_0 + \rho_l V_p.$$

As was shown by the experimental data, porous specimens saturated with different liquids under the same conditions had different degrees of filling, i.e., we obtained different values of V_p. The greatest volume V_p was obtained for a specimen filled with ethyl ether and the least was obtained for a specimen filled with mercury. It can thus be seen from these experiments that not all the pores were filled to an equal extent with different liquids.

In order to get an idea of the real structural pattern of a cermet porous specimen, we made a photomicrograph (enlarged 120 times) of a cross section of the specimen (Fig. 3). The photomicrograph quite clearly shows the complex structure of the internal surface of the porous element, which had open and closed pores, macropores and micropores, randomly structured communicating and noncommunicating pores, and interconnections of irregular form. Moreover, there were small areas with the more or less regular packing characteristic of aggregates of grains well segregated for uniform size. Since all these pores composed the total pore space, we determined the total, or absolute, porosity statistically, in addition to the porosity

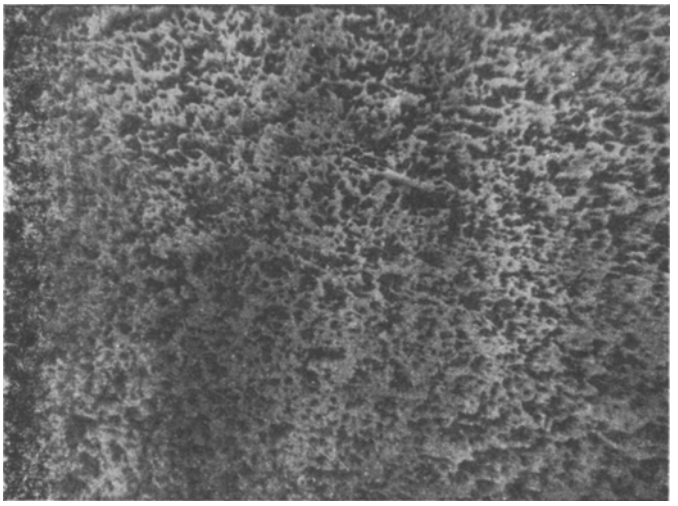

Fig. 3. Photomicrograph of cross section of specimen.

characterizing the communicating pores. The total porosity of the element was greater than its active porosity by approximately 5%.

As can be seen from the photomicrograph, the porous element consisted of a system of pores with a certain size distribution. The structural complexity of a porous material does not permit precise determination of the "pore size," but use of the statistical method makes it possible to represent the pore distribution graphically on the basis of average size. The number of pores whose average size lies in the interval between r and r + dr is represented by the area of the shaded trapezoid in Fig. 4. The entire area lying between the graph and the abscissa is numerically equal to the average number of pores per unit area.

In order to establish this relationship, a photomicrograph of an element section, made at a magnification of 120 times, was cut into identical squares. The total number of pores in each square was counted and their average size was determined with a microscope fitted with an ocular micrometer. This method made it possible to determine the average number of pores in each square and to divide them into groups on the basis of their average size.

Microphotography of an element section at a magnification of 1000× showed the presence of a large number of smaller pores and microcracks, but it was virtually impossible to count them or evaluate their size, so that they are not represented in the graph. It can be seen from Fig. 4 that the maximum of the curve for $dn_0/dr = f(r)$ was displaced toward the micropore region. This also gives us grounds for surmising that cermet elements contain a large number of pores whose average diameter is less than 10^{-5} cm.

Analysis of the relationship $\lambda_{ef}/\lambda_{sk} = f(P)$ (Fig. 5) showed that it was observed for most gases only in the region of pressures $P < 15{,}960\ N/m^2$ ($P < 120$ mm Hg). Helium was an exception, with this relationship developing at $P < 5 \cdot 10^4\ N/m^2$ ($P < 350$ mm Hg). When the specimen was filled with water vapor, the relationship $\lambda_{ef}/\lambda_{sk} = f(P)$ appeared at $P < 1 \cdot 10^4\ N/m^2$ ($P < 80$ mm Hg), while the range for freon was $P < 8 \cdot 10^3\ N/m^2$ ($P < 60$ mm Hg). The effective coefficient of thermal conductivity was independent of the filler-gas pressure at $P > 15{,}960\ N/m^2$ but, as can be seen from Fig. 5, depended strongly on the properties of the gas. The greatest thermal conductivity was exhibited by the specimen filled with water vapor and the least by that filled with dry air. The specimen filled with freon had a somewhat greater thermal conductivity than that filled with dry air, although the thermal conductivity of freon itself is less than that of dry air by a factor of about two.

Proceeding from the theory of thermal conductivity, the coefficient of thermal conductivity of a porous system under vacuum conditions should be governed solely by the thermal conductivity of the framework material, taking into account the contact thermal resistance. As our experimental data show, however, the effective thermal conductivity of the specimens at $P > 1\ N/m^2$ was not the same in experiments with different gases, differing by an amount several orders of magnitude greater than the thermal conductivity of the gas at the pressure in question.

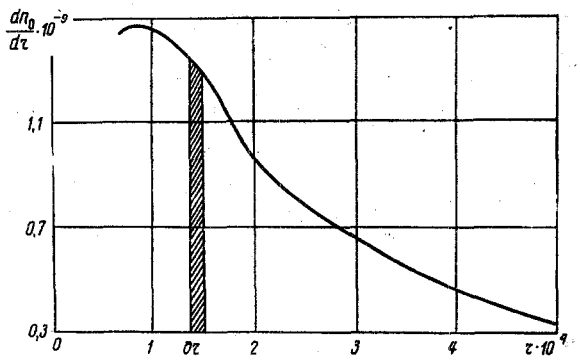

Fig. 4. Pore distribution by average size.

We will consider the effective thermal conductivity of a porous system as a function of the porosity, the thermal conductivity of the gas filling the material pores, the thermal conductivity of the gas microspaces, the contact thermal conductivity between the particles, and the thermal conductivity of the particles themselves. Convection in the pores and radiation are neglected, since the pores are small in size and the temperature difference between the hot and cold sides of the plate did not exceed 2°:

$$\frac{\lambda_{ef}}{\lambda_{sk}} = f\left(\Pi;\ \frac{\lambda_g}{\lambda_{sk}};\ \frac{\lambda_{g.s}}{\lambda_{sk}};\ \frac{\lambda_c}{\lambda_{sk}}\right). \tag{3}$$

On the basis of the molecular–kinetic theory of gases, the thermal conductivity of the gas filling the material pores was determined as a function of the average arithmetic molecular velocity w_m, the mean free molecular path Λ, the isochoric heat capacity c_V, the gas density, and the adiabatic index k, i.e.,

$$\lambda_g = 0.499\,\frac{9k-5}{4}\,w_M \Lambda c_v \gamma. \tag{4}$$

Since the thermal conductivity of the framework of a cermet porous system is greater than that of the filler gas by more than two orders of magnitude, the second component in Eq. (3) can be neglected, because of its smallness, and we can concentrate our attention on the thermal conductivity of the gas microspaces and the content thermal conductivity between the particles.

The thermal conductivity of a porous system depends on the contact area between the particles, which are linked by contact bridges or spots with different cross sections in real systems containing all possible defects and microspaces.

Part of the heat flux in the region of interparticle contact passes through the microspaces, while part of it goes through the sites of direct particle linkage. As numerous studies have shown, the contact thermal resistance is a direct function of the fabrication procedure for porous members, i.e., the pressure under which the metal powder is pressed, the sintering temperature, the purity and physical properties of the particle material, etc.

If the sintering temperature of the powdered metal is close to its melting point, there is local fusion of the microprotuberances on the particles to form an integral porous cermet system. The contact thermal resistance at the junctions in such a system becomes negligibly small. If the sintering temperature of the cermet system is below the melting point of the metal, possible partial sintering of individual grains can occur. In this case, the thermal contact resistance of porous cermet materials can be represented as the sum of two components:

$$R_c = R_L + R_0, \tag{5}$$

and the contact thermal conductivity is

$$\lambda_c = \frac{1}{R_c F_c}. \tag{6}$$

The quantity R_L is the thermal resistance due to reduction of the cross-section for the thermal flux passing through the contacting particles. For most porous systems,

$$R_L \cong \frac{b}{2r_s\lambda_{sk}}, \tag{7}$$

where b is the coefficient that takes into account the reduction in cross-section for the heat flux; it is close to one for most granular porous systems (b ≈ 1-1.2). The radius of the contact spot r_s depends on the pressure and, in a rough first approximation, can be determined from the Hertz formula

$$r_s = 0.725\sqrt[3]{\eta PL/2}, \tag{8}$$

where

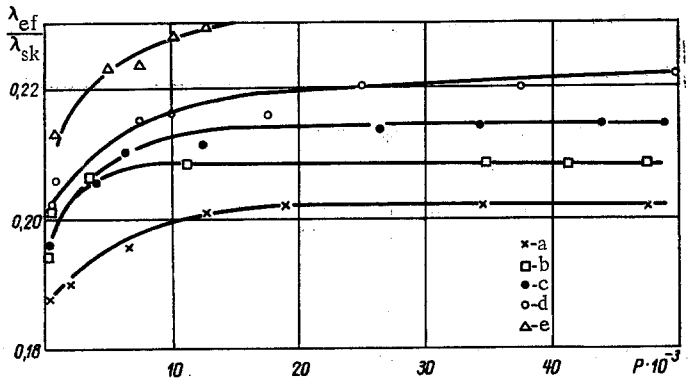

Fig. 5. Relative effective coefficient of thermal conductivity of titanium element $\lambda_{ef}/\lambda_{sk}$ as a function of filler-gas pressure P (n/m^2): a) dry air; b) freon-12; c) damp air (moisture content of 70%); d) helium; e) water vapor.

$$\eta = \frac{2(1-\mu^2)}{E}.$$

The quantity R_0 is the thermal resistance to the heat flux due to the presence of oxide films on the metallic particles. Little research has been done on its influence on the effective thermal conductivity of porous cermet systems. As a result of the large number of governing factors, such as the physical properties of the material, the pressing pressure, the sintering temperature, the cleanness of the particle surface, the type of atmosphere in which sintering takes place, etc., the contact resistance is thus not accessible to analytic calculation from any single standpoint. The true contact resistance of a porous system can only be determined experimentally. For example, if the thermal conductivity of a porous system under vacuum conditions is known, the contact resistance can be calculated from the difference between the experimental and calculated data.

Analyzing the function $\lambda_{ef}/\lambda_{sk} = f(P)$, we can conclude that the difference in the values of λ_{ef} is apparently caused by filling of the microspaces between the grains and the microcracks in the grains themselves with gas.

This increase in λ_{ef} at different pressures is considerably greater than the values of λ predicted from the thermal conductivity of the gas on the basis of the molecular–kinetic theory. The difference between the experimental and calculated values of $\lambda_{g.s.}$ can only be attributed to adsorption of the gas by the porous material, especially at the contact sites and grain defects. In this case, the amount of adsorbed gas increases with the pressure; the gas molecules are adsorbed on the free surface of the micropores of the porous system, forming molecular films. If the adsorbed molecules do not completely cover the surface of the micropores, they can have some mobility on the surface, forming a "two-dimensional" gas. As the number of molecules in a condensed gas increases, i.e., the pressure rises, they can condense to form a "two-dimensional" liquid.

Since the thermal conductivity of a liquid layer is far greater than that of a gaseous layer, the λ_{ef} of a porous element filled with water vapor is higher than that of a specimen filled with an inert gas, although the thermal conductivity of helium and air is known to be greater than that of water vapor.

In porous systems not capable of a chemical interaction with the gas, the gas molecules are adsorbed by the porous solid by virtue of purely physical forces. These are weaker polarizational forces similar to those that cause compression of gases.

Physical adsorption increases as the temperature is reduced; at constant temperature, those gases that are more readily condensed, i.e., have higher boiling points, are adsorbed best.

It can be seen from our experiments that the amount of gas adsorbed at constant temperature increased very rapidly as the pressure was raised to $1 \cdot 10^4$ N/m^2 and then tended to a certain constant limit as the pressure was further increased, i.e., when a layer of adsorbed gas of definite thickness was formed at the grain contact sites and in the microspaces, an increase in pressure had no effect on the value of λ_{ef}.

We conducted special experiments on adsorption in porous cermet elements by the gravimetric method in order to verify the hypothesis that physical adsorption affects the value of λ_{ef}.

During these experiments, a porous specimen was placed in a hermetically sealed glass dish, which was connected to a vacuum system and simultaneously heated to high temperature. After vacuum degassing of the porous element, the glass dish was disconnected from the vacuum system and connected to the gas-delivery system; it was then placed on an analytic balance. The change in element weight (taking into account the weight of the gas in the specimen pores and in the dish) at definite temperatures and pressures showed the porportion of the total weight involved in adsorption during filling of the porous specimens with various gases.

The weight of the adsorbed gas was calculated from the equation

$$M = m + \rho_g V_a - m_0.$$

The amounts of gas adsorbed were found to differ during filling of a porous specimen with different gases. The highest values of M were obtained by filling porous specimens with water vapor.

It must be noted that the adsorption rate depends not only on the ambient pressure and temperature but also on the ratio of the diameters of the gas molecules and microspaces. Since any porous system has pores of all possible sizes, including micropores of molecular size, the presence of such pores in the system has a strong influence on λ_{ef}, since they can be completely filled with adsorbed gas.

Sorption of water vapor has a different character from that of other gases. For example, electronic measurements showed the thickness of the adsorbed film under normal conditions to be considerably greater for water vapor than for other gases. Water vapor can condense to a liquid in the micropores and microspaces.

On the basis of the experimental data for the pressure region $P < 16{,}000$ n/m^2, the difference between λ_{ef} and λ due to the influence of gas adsorption in the microspaces can be described by a parabolic equation of the type

$$\frac{\lambda_{g.s}}{\lambda_{sk}} \sim \frac{\lambda_{ef} - \lambda}{\lambda_{sk}} = AP^n, \tag{9}$$

where the power n is approximately 0.176 for all gases, while the coefficient A depends on the type of filler gas and takes the following values: $11.2 \cdot 10^{-3}$ for water vapor, $2.7 \cdot 10^{-3}$ for helium, $7.9 \cdot 10^{-3}$ for damp air, $7.8 \cdot 10^{-3}$ for freon, and $4.8 \cdot 10^{-3}$ for dry air.

NOTATION

λ_{sk} is the coefficient of thermal conductivity of porous material skeleton;
λ is the coefficient of thermal conductivity of porous material in vacuum;
λ_{ef} is the effective coefficient of thermal conductivity of porous material;
c_p is the heat capacity;
a is the coefficient of temperature conductivity;
Q is the heat flux;
Π is the active porosity;
δ is the specimen thickness;
D is the diameter;
P is the pressure;
μ is the Poisson's constant;
E is the modulus of elasticity;
M is the weight of adsorbed gas;
m is the weight of porous element with adsorbed gas;
m_0 is the weight of element in vacuum;
ρ_g is the gas density in element pores;
V_a is the total active volume of element pores;
M_l is the mass absorbed by porous specimen;
ρ_l is the density of liquid;
V_p is the volume of open pores;
n_0 is the number of pores.

LITERATURE CITED

1. A. V. Lykov, Theoretical Principles of Structural Thermophysics [in Russian], Izd. Akad. Nauk BSSR (1961).
2. G. N. Dul'nev and Z. V. Sigalov, Inzh.-Fiz. Zh., 7, No. 10 (1964).
3. L. L. Vasil'ev and Yu. E. Fraiman, Thermophysical Properties of Poor Heat Conductors [in Russian], Nauka i Tekhnika, Minsk (1967).
4. K. U. Besserer, Engineering Handbook for Guided Missiles [in Russian], Voenizdat, Moscow (1962).
5. A. Missenard, Conductivite Thermique des Solides, Liquides, Gas et de Leurs Milanger, Paris (1965).